PROCEEDINGS OF SPIE

Seventh European Workshop on Optical Fibre Sensors

Kyriacos Kalli
Gilberto Brambilla
Sinéad O'Keeffe
Editors

1–4 October 2019
Limassol, Cyprus

Organized by
Cyprus University of Technology (Cyprus)

Sponsored by
OZ Optics Ltd. (Canada)

Cooperating Organization and Publisher
SPIE

Volume 11199

Proceedings of SPIE 0277-786X, V. 11199

The papers in this volume were part of the technical conference cited on the cover and title page. Papers were selected and subject to review by the editors and conference program committee. Some conference presentations may not be available for publication. Additional papers and presentation recordings may be available online in the SPIE Digital Library at SPIEDigitalLibrary.org.

The papers reflect the work and thoughts of the authors and are published herein as submitted. The publisher is not responsible for the validity of the information or for any outcomes resulting from reliance thereon.

Please use the following format to cite material from these proceedings:
Author(s), "Title of Paper," in *Seventh European Workshop on Optical Fibre Sensors (EWOFS 2019)*, edited by Kyriacos Kalli, Gilberto Brambilla, Sinead O. O'Keeffe, Proceedings of SPIE Vol. 11199 (SPIE, Bellingham, WA, 2019) Seven-digit Article CID Number.

ISSN: 0277-786X
ISSN: 1996-756X (electronic)

ISBN: 9781510631236
ISBN: 9781510631243 (electronic)

Published by
SPIE
P.O. Box 10, Bellingham, Washington 98227-0010 USA
Telephone +1 360 676 3290 (Pacific Time) · Fax +1 360 647 1445
SPIE.org

Printed in the United States of America by Curran Associates, Inc., under license from SPIE.

Publication of record for individual papers is online in the SPIE Digital Library.

SPIE. DIGITAL LIBRARY
SPIEDigitalLibrary.org

Paper Numbering: *Proceedings of SPIE* follow an e-First publication model. A unique citation identifier (CID) number is assigned to each article at the time of publication. Utilization of CIDs allows articles to be fully citable as soon as they are published online, and connects the same identifier to all online and print versions of the publication. SPIE uses a seven-digit CID article numbering system structured as follows:

- The first five digits correspond to the SPIE volume number.
- The last two digits indicate publication order within the volume using a Base 36 numbering system employing both numerals and letters. These two-number sets start with 00, 01, 02, 03, 04, 05, 06, 07, 08, 09, 0A, 0B … 0Z, followed by 10-1Z, 20-2Z, etc. The CID Number appears on each page of the manuscript.

Astigmatism compensation for waveguide inscription in optical fiber by femtosecond lasers

D. Pallarés-Aldeiturriaga[a,b], P. Roldán-Varona[a] L. Rodriguez-Cobo[b] and J.M. Lopez-Higuera[a,b,c]

[a]Photonics Engineering Group, University of Cantabria, 39005, Santander (Spain);
[b]CIBER-bbn, Instituto de Salud Carlos III, 28029, Madrid (Spain);
[c]Instituto de Investigación Sanitaria Valdecilla (IDIVAL), Cantabria, Spain.

ABSTRACT

The cylindrical geometry of optical fibers produces an astigmatic distortion in a wavefront focused within it. In the case of femtosecond lasers, this produces a fluence loss that decreases its processing performance. In this work, the phase change produced by an astigmatic femtosecond laser beam (direct exposition to the) and a corrected beam (applying a simple adaptive optics process) is compared. The astigmatic correction decreases the modification threshold by approximately a magnitude order and changes the sign of the refractive index change at low pulse energies.

Keywords: Femtosecond lasers, waveguides, optical fibers, gaussian beams.

1. INTRODUCTION

Femtosecond (fs) lasers play a vital role in the manufacture of Optical Fiber Sensors (OFS), producing optimized and compact designs. It allows inscription of fiber Bragg gratings (FBGs) without requiring a photosensitive optical fiber, withstanding high temperature [1] and its combination with chemical etching can create microfluidic channels or microcavities [2, 3]. In addition, another remarkable application is waveguide inscription; this is not only a versatile tool to develop compact in-fiber interferometers [4] but also a way to connect different transducer elements on the same fiber, creating complex lab on fiber devices [5].

The major difficulty of waveguide inscription in optical fibers is its cylindrical geometry that induces significant astigmatism on the focal volume, thus decreasing laser fluence. This issue can be addressed by oil immersion but requires a particular microscope objective. Zhou *et al.* has proposed another method to suppress this astigmatism that does not require such objectives [2]. It has been employed for microfluidic (assisted by wet etching) and FBG inscription. However, this method also exhibits interest in waveguide inscription. In this work, the role of astigmatism induced by optical fiber geometry in the power distribution is reviewed and the phase (proportional to Refractive Index (RI)) change of inscriptions employing astigmatic correction is studied and compared with direct exposition at the fiber core.

2. FOCUSING ON AN OPTICAL FIBER

When a laser pulse (with a wavelength λ) is focused through a numerical aperture (NA) microscope objective (in a background index n_0) to a planar dielectric sample (with Refractive Index (RI) n_{cl}) its waist width ω_0 and Rayleigh range z_R are [1] :

$$\omega_{0p} = \lambda/(NA\pi), \quad z_{Rp} = \lambda n_{cl}/(\pi NA^2). \tag{1}$$

This planar index change already induces a displacement on the focal point perpendicular to the RI quotient $n = n_{cl}/n_0$ in the paraxial region. The focal point is displaced to $z' = nz$ (paraxial approximation), where z is the distance from the interface to the focal point in n_0. In the most majority of fs laser applications, a high NA is employed. However, for these NAs, the paraxial approximation is no longer valid, and ray trajectories with a higher angle will focus below paraxial approximation (spherical aberrations). Thus, there is a defocusing

Corresponding author: David Pallarés Aldeiturriaga (david.pallares@unican.es).

Seventh European Workshop on Optical Fibre Sensors, edited by Kyriacos Kalli, Gilberto Brambilla, Sinead O'Keeffe
Proc. of SPIE Vol. 11199, 111992T · © 2019 SPIE · CCC code: 0277-786X/19/$21 · doi: 10.1117/12.2539835

proportional to the penetration depth and displacement of the focal point. Such loose of focusing is depicted in Fig. 1a for a $\lambda = 1030nm$ light source focused through a NA=0.5 lens in air and a dielectric medium $n_{cl} = 1.45$ with its interface placed $30\mu m$ above focal spot in air.

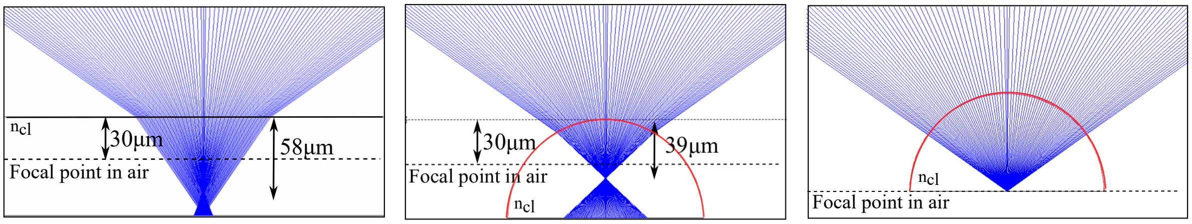

(a) (b) (c)

Figure 1: Ray trace of a NA=0.5 microscope lens focused in: planar object $n_{cl} = 1.45$, $30\mu m$ above working distance (a), circular object of same RI at same position (b) and matching working distance with object center (c).

When the incident light comes across a circular geometry, it experiences the common focusing expected from a lens. For example, if the planar surface from Fig. 1a were substituted by a circular surface with $125\mu m$ diameter, the focal spot would displace $9\mu m$ below, as depicted in Fig. 1b. The special case comes when the focal spot and the circumference center matches. Now all the rays are perpendicular to the circumference surface; thus, there is no focal displacement (Fig. 1c). The gaussian waist and Rayleigh range are [1]:

$$\omega_{0c} = \lambda/(n_{cl} NA\pi), \quad z_{Rc} = \lambda/(n_{cl}\pi NA^2). \tag{2}$$

When a gaussian beam is focused within an optical fiber, the axis parallel and perpendicular to the axis will exhibit different parameters, behaving as an orthogonal astigmatic beam. The intensity distribution for a simple astigmatic gaussian beam with a beam power P, is [6]:

$$I = \frac{2P}{\pi\omega_x(z)\omega_y(z)} e^{-2\left(\left(\frac{x}{\omega_x(z)}\right)^2 + \left(\frac{y}{\omega_y(z)}\right)^2\right)}, \tag{3}$$

$$\omega_i(z) = \omega_{0i}\sqrt{1 + \left(\frac{z - z_{0i}}{z_R}\right)^2}. \tag{4}$$

If one compares the beam intensity at the center along z direction of an astigmatic beam produced by an optical fiber and a stigmatic beam produced by a planar sample, the latter will exhibit higher intensity concentrated in a lower region. This is depicted in Fig. 2a for the parameters above. The intensity of the astigmatic beam exhibits two maximums corresponding to the two minimal waist position while stigmatic intensity distribution exhibits only one maximum with a magnitude order higher than the astigmatic maximum. Fig. 2b shows the focal volume of stigmatic and astigmatic beams at different intensities normalized to the stigmatic maximum. Note that astigmatic focal volume does not contain intensities higher than the normalized 10%, requiring higher laser pulse energies to perform modifications to the material. Thus, increasing its modification threshold.

3. INSCRIPTION SETUP

Waveguide inscription was performed by a conventional transversal writing setup. A femtosecond laser chirped pulse amplifier (FLCPA) from Calmar laser ($\lambda = 1030nm$, $\tau = 370fs$, 120kHz) was employed. Lasers were focused through an aspheric objective lens x100/NA=0.5 from Mitutoyo through a conventional SMF-28 placed in a nano resolution movable stage from Aerotech. This stage was also illuminated to capture light with the same objective and monitor the inscription with a CCD camera.

In order to remove astigmatism in the focal volume, the scheme introduced by Zhou *et al.* was employed [2]. This scheme mainly consists of a drop of index matching oil surrounding the fiber sandwiched by a slide and a coverslip.

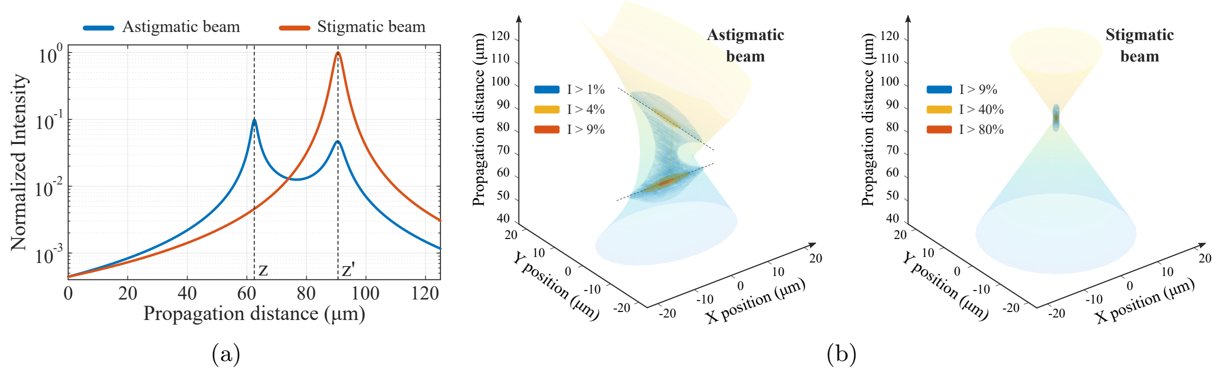

Figure 2: Intensity distribution with propagation distance along the material at the beam center for stigmatic and astigmatic beams (a), the intensity has been normalized to the stigmatic maximun. Focal volume representation of both beams (b), astigmatic focal volume does not contain intensities higher than the normalized 10%.

4. PHASE RESULTS

The effect of astigmatism removal is notorious from Fig. 3a where two intensity images of inscribed lines with $0.47\mu J$ (0.1mm/s) pulse energy are depicted. The width of the pattern inscribed with direct exposition is significantly lower than its adaptive optics counterpart. Also, the modification is smooth, without distinctive sharp details proper of high fluence inscriptions.

For a more quantitative approach, phase change was retrieved by Quantitative Phaser microscopy (QPm). This method retrieves a phase image employing the intensity transport equation from a set of defocused intensity images [7]. These images were obtained through the same CCD camera and microscope objective from the inscribing setup with $\pm 3\mu m$ defocusing. Several lines at pulses energies ranging from 0-2.5 μJ were inscribed at 0.1mm/s with and without astigmatic correction. The result is depicted in Fig. 3b, where the first phase changes are produced at $0.06\mu J$ with adaptive optics while direct exposition requires $0.67\mu J$. This is approximately a factor 10 estimated from Fig. 2a. The most notorious feature between the two types of the inscription is its sign. Astigmatic beams produce a negative change while circular beam produces positive phase change. This inscription exhibits four regions. The first one ranges from 0-$0.31\mu J$ and is characterized for a smooth, positive Type I Refractive Index Change (RIC). From 0.31-$0.67\mu J$, the width of the lines increases, exhibiting an exterior region with high phase change and an interior region of lower phase change. Comparing phase images of first ($0.09\mu J$) and second ($0.47\mu J$), the inscription is brighter (more phase change), and its width ($2.5\mu m$) corresponds with the central part of the second region. With higher pulse energies, the structure becomes more complex. Positive change predominates despite forming secondary structures with a negative index. Filamentation is likely to occur at this regime. For pulse energies higher than $1.09\mu J$, the pulse damages the coverslip inducing a measuring error in the phase change.

Direct exposure, on the other hand, produces negative index change thinner than its corrected counterpart. First, there is a smooth negative RIC until $1.09\mu J$; from this value, the focal volume experiences an abrupt negative phase increase up to stabilize at $1.97\mu J$ and then it decreases monotonically. The inscribed lines in this region exhibit filamentation with a filament length greatly dependent on the writing speed. These filaments can exhibit positive RIC, being able to guide light. In addition to the inscription with and without astigmatism correction at fiber core, another set of inscriptions focused $30\mu m$ below fiber surface were performed. Here the degree of astigmatism is significantly lower, allowing high phase change $0.31\mu m$ (bellow modification threshold for same parameters focused at the core). These phase change, however, remains relatively stable with laser fluence. Filamentation occurs along all the region and with lengths higher than its core counterpart.

From the discussion above, it is clear that astigmatism correction not only reduces the modification threshold but also allows smooth Type I RICs that would not be possible otherwise. These changes are useful for waveguide inscription (more specifically for multiscan inscription) and grating inscription.

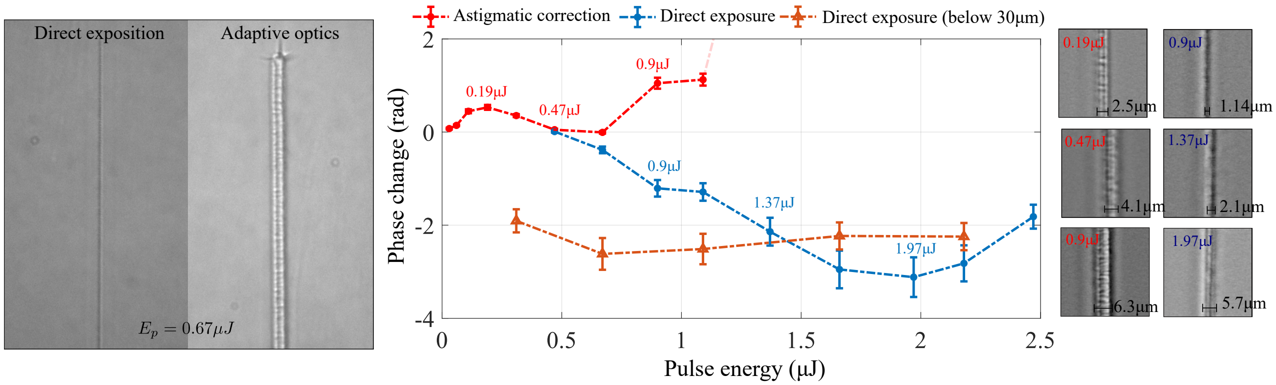

(a) (b)

Figure 3: Inscription with and without adaptive optics at $0.67\mu J$ (a). Phase change vs pulse energy for inscribed lines with and without adaptive optics focused at the fiber core and also $30\mu m$ below surface without adaptive optics (b). Some relevant phase images for the core inscriptions are also depicted.

5. CONCLUSIONS

In this work, it is presented a detailed study on the beam astigmatism induced when fs laser pulses are focused within an optical fiber. A simple method for its correction has been employed, and its effect on phase change has been studied. Results suggest that astigmatism correction reduces modification threshold by approximately a magnitude, which it is coherent with previous calculations. Lines inscribed at low fluence with this correction exhibits a positive Type I change. These modifications are useful for waveguide and grating inscription.

ACKNOWLEDGMENTS

This work has been supported by the project TEC2016-76021-C2-2-R (AEI/FEDER, UE) and grants BES-2014-069736 from Ministerio de Economía y Competitividad.

References

[1] J. Thomas, C. Voigtländer, R. G. Becker, D. Richter, A. Tünnermann, and S. Nolte, "Femtosecond pulse written fiber gratings: A new avenue to integrated fiber technology," *Laser and Photonics Reviews* **6**(6), pp. 709–723, 2012.

[2] K. Zhou, F. Shen, G. Yin, and L. Zhang, "Optical fiber micro-devices made with femtosecond laser," in *Advanced Photonics Congress*, p. SeW3D.1, Optical Society of America, 2016.

[3] A. K. Dębowska, M. Koba, M. Janik, W. J. Bock, and M. Śmietana, "Increased sensitivity of femtosecond laser micro-machined in-fiber Mach-Zehnder interferometer for small-scale refractive index sensing," in *Sixth European Workshop on Optical Fibre Sensors*, **9916**, p. 99160Q, 2016.

[4] D. Pallares-Aldeiturriaga, L. Rodriguez-Cobo, A. Quintela, and J. M. Lopez-Higuera, "Curvature Sensor Based on In-Fiber Mach-Zehnder Interferometer Inscribed with Femtosecond Laser," *Journal of Lightwave Technology* **35**(21), pp. 4624–4628, 2017.

[5] Moez Haque, *Chemical-Assisted Femtosecond Laser Writing of Lab-in-Fiber Sensors*. PhD thesis, University of Toronto, 2014.

[6] E. Kochkina, *Stigmatic and Astigmatic Gaussian Beams in Fundamental Mode Pathlength Signal Estimates*. PhD thesis, Leibniz Universität Hannover, 2013.

[7] C. J. Bellair, C. L. Curl, B. E. Allman, P. J. Harris, A. Roberts, L. M. Delbridge, and K. A. Nugent, "Quantitative phase amplitude microscopy IV: Imaging thick specimens," *Journal of Microscopy* **214**(1), pp. 62–69, 2004.